ACS APPLIED POLYMER MATERIALS

Article

Cite This: ACS Appl. Polym. Mater. 2019, 1, 425−436

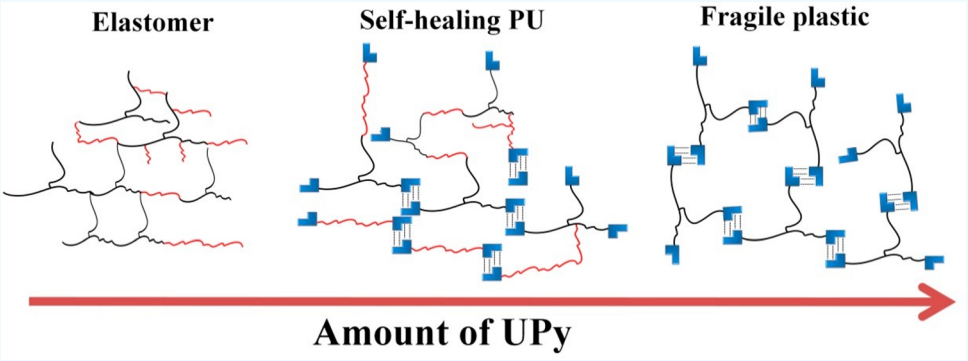
pubs.acs.org/acsapm

From Fragile Plastic to Room-Temperature Self-Healing Elastomer: Tuning Quadruple Hydrogen Bonding Interaction through One-Pot Synthesis

Yanxiong Pan,[‡] Jinlian Hu,*[,‡] Zhongyu Yang,[†] and Lin Tan[‡]

[†]Department of Chemistry and Biochemistry, North Dakota State University, Fargo, North Dakota 58108, United States

Supporting Information



ABSTRACT: Self-healing polymers are attractive smart materials finding applications in many fields. Most of these materials often need feeding of reagents as supplements or require external stimuli to induce the healing of damage zone. An attractive alternative is the polymeric materials based on hydrogen bonding which allow for room-temperature self-healing with no need of supplement feeding. However, most of these materials possess poor mechanical properties, which limit their practical application. Here we use a one-pot synthesis strategy to prepare a series of H-bonding based smart polyurethanes (PUs) with tunable self-healing and mechanical properties. These PUs were prepared from PEG-diol and PPG-triol with ureidopyrimidinone (UPy) motifs incorporated in the polymer matrices via reaction between isocyanate and 2-amino-4-hydroxy-6-methylpyrimidine (AHMP). Attenuated total reflectance-Fourier transform infrared (ATR-FTIR) spectroscopy confirms the successful preparation of PUs. Thermal analysis reveals that upon introduction of UPy motifs in the PU network the crystallinity of the PEG part was destroyed due to the formation of urethane bonds with isocyanate, while the thermal stability of PUs was only slightly decreased. Destroying the PEG crystals increases the durability of the materials. Furthermore, the T_g of our PUs can be adjusted by the contents of AHMP and PPG. At low and moderate contents of AHMP, the T_g was < −20 °C. As the content of AHMP was increased, T_g was increased and eventually disappeared. Also, T_g was slightly decreased with an increase in PPG. This feature is highly desirable for designing PU with tunable mechanical properties ranging from fragile plastics to strong elastomers with excellent room-temperature self-healing capabilities. More importantly, these materials can be prepared under mild conditions and have the advantages of non-cross-linking network, excellent mechanical properties, and rapid and repeatable self-healing properties, which make these materials ideal candidates for "smart" applications.

KEYWORDS: *polyurethane, elastomer, room-temperature self-healing, Upy, multiple hydrogen interaction*

Downloaded via NORTH DAKOTA STATE UNIV on May 11, 2019 at 04:15:39 (UTC).
See https://pubs.acs.org/sharingguidelines for options on how to legitimately share published articles.

1. INTRODUCTION

Over the last several decades, researchers have witnessed the development and achievement of smart materials based on polymers due to the progress in synthesis strategies and characterization technologies.[1−3] Among the various types of smart polymers or polymeric composites, the self-healing polymers attract great interest due to their capability of self-repairing the mechanical fractures and extending their lifetimes.[4−7]

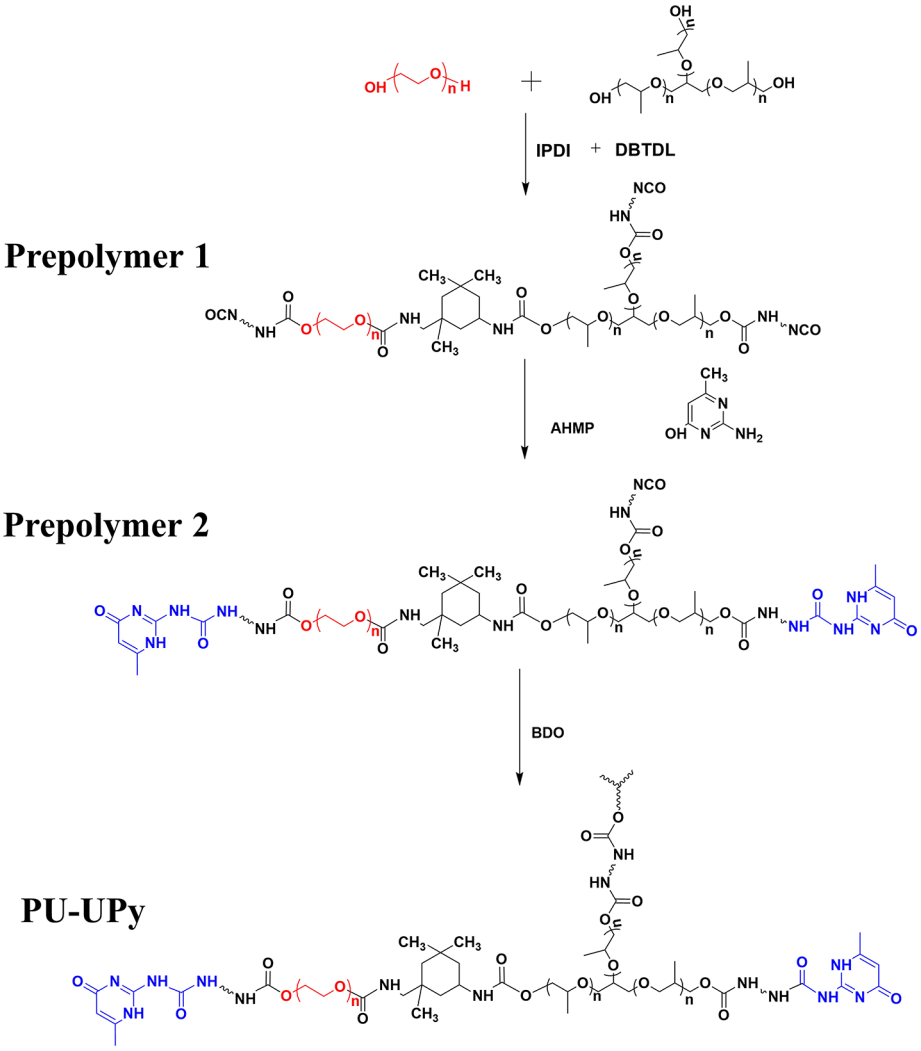
In comparison to regular polymeric materials, self-healing materials have the advantages of reversing the damage, suppressing microcrack, and relatively longer life cycles because their broken parts or cavities formed by damage could be recovered automatically. These advantaged materials exhibit a broad spectrum of applications such as shape memory materials,[8−10] stretchable organic electronics,[11,12] paints,[13,14] and other applications.[3,15,16] Inspired by nature, most self-healing materials were designed based on two primary approaches, extrinsic and intrinsic self-healing, to realize the automatic recover of damage zone.[1] For the extrinsic self-healing, the regents (including liquid and solid regent) for healing, which are separately incorporated into the micro-

Received: November 20, 2018
Accepted: February 5, 2019
Published: February 5, 2019

© 2019 American Chemical Society

DOI: 10.1021/acsapm.8b00153
ACS Appl. Polym. Mater. 2019, 1, 425−436

Scheme 1. Schemes of Preparation of PU Containing UPy Motifs via Random Coupling of PEG, PPG, AHMP with IPDI



encapsulation,[17,18] hollow glass fiber[19] and channels,[20] could be automatically released and heal the damage position once crack appearance. In contrast, no extra chemistries are needed in the intrinsic self-healing, which realizes self-healing via forming and breaking reversible covalent bonds or noncovalent bonds.[1,4,6] So far, intrinsic self-healing materials with various components and self-healing mechanisms have been developed such as covalent bonding,[21,22] supramolecular network,[23−27] polymer−metal ion system,[28−32] metal−ligand coordination,[29] disulfide metathesis,[33−36] etc.[27,37−41] Most of the intrinsic self-healing polymers or polymeric composites show relatively good mechanical property; their self-healing relies on external stimuli, such as light,[42] heat,[43,44] magnetic,[45] even water molecular,[40,46] to carry out the self-healing function because extra energy is required for the motion of polymer chain to heal the broken parts via reversible chemical and physical bonds. For the samples to hold room-temperature self-healing properties, the relatively weaker mechanical property is be the biggest obstacle for their practical applications.

A promising alternative self-healing mechanism to avoid the need of supplying reagents or energy is via hydrogen bonding,[26,46−50] which plays an important role in polymers in determining their morphology and function as well as mechanical properties.[51,52] Quadruple hydrogen bonding motifs have been incorporated to prepare polymers with unique reversibility and temperature dependent rheology for two decades.[53−56] Polymers developed using this approach include thermoreversible polymers,[57] supramolecular architectures,[58,59] light healable supramolecules,[60] crystalline supramolecules,[61] even flexible and printed nanocarbon electrodes.[62] Most of these materials rely on the UPy moiety, which can be incorporated to polymers via step synthesis[53] or reaction between isocyanate and 2-amino-4-hydroxy-6-methylpyrimidine (AHMP).[63−65] The resultant products containing the UPy motifs at the end of chains endowed the materials with relatively stronger mechanical properties. Although these materials do not need extra supply of reagents, the self-healing reaction still requires external stimuli such as thermal energy[66,67] and light.[60,68] Room temperature self-healing materials based on H-bonding are also available.[26,46−48,69−72] However, these materials often suffer from inherent deficiencies such as complicated procedures of preparation, reduced mechanical properties, and relatively high cost, which hinder their practical applications. Therefore, a self-healing material with simpler preparation procedures and stronger mechanical properties is still needed in the field of self-healing materials.

DOI: 10.1021/acsapm.8b00153
ACS Appl. Polym. Mater. 2019, 1, 425−436

In this work, we report a one-pot chemical synthesis method for preparing UPy motif containing polyurethane (PU). The mechanical properties of as-prepared PUs can be tuned by adjusting the feeding ratio of AHMP, making either fragile plastics or self-healing elastomers. Remarkably, the PUs with moderate amount UPy motif display excellent room-temperature self-healing performances as well as relatively good mechanical properties. This is the first report on smart polymers, which simultaneously address the needs of room-temperature self-healing and mechanical strength.

2. EXPERIMENTAL SECTION

2.1. Materials. The polyethylene glycol (PEG-diol M_n = 1000) was purchased from SK chemical, and poly(propylene glycol)s (PPG-triol M_n 3000) were purchased from Chinese National Offshore Oil Corporation (CNOOC) and Shell Petrochemicals Company Limited (CSPC). Isophorone diisocyanate (IPDI, 98%) was purchased from Degussa Vestana. 2-Amino-4-hydroxy-6-methylpyrimidine (AHMP, 98%), 1,4-butanediol (BDO, 99%), and dibutyltin dilaurate (DBTDL, 95%) were purchased from Sigma-Aldrich, and N,N-dimethylformamide (DMF, HPLC grade) was purchased from Duksan Pure Chemicals. All chemicals purchased from the commercial suppliers were used without further purification,

2.2. Preparation of Self-Healing PU Elastomer. Preparation of prepolymer was adapted from a previously described solution polymerization protocol.[58] Typically, PPG 3000 and PEG 1000 were mixed with various ratios (see Table S1) in a two-necked bottle under vigorous stirring. The degas process was carried out by warming up the mixture to 85 °C under vacuum for 2 h. Then IPDI (8.339 g, 37.5 mmol) and DBTDL (5 mL, 7.3 mmol. L^{-1} (solute in the DMAc)) were added into the PPG/PEG mixture for 2 h to prepare the prepolymer whose ends were capped with isocyanate groups. Thereafter, AHMP was added under vigorously stirring for 30 min to obtain a clear solution, and subsequently preprepared BDO (0.923 g, 20.5 mmol) was mixed with the above mixture and poured into the Teflon mold and incubated in oven at 100 °C for 12 h. The final product is the PU1/*n*-AHMP-m, where *n* is the molar ratio of −OH hydroxyl group of PEG-diol to PPG-triol while m is the molar ratio of the total −OH and $-NH_2$ groups from AHMP to the total −OH groups from PEG-diol and PPG-triol. Details are listed in Table S1.

2.3. Characterization. FTIR spectroscopy was performed on a BRUKER Vertex 70 spectrometer equipped with attenuated total reflection (ATR). Thermal properties of samples were characterized using differential scanning calorimetry (DSC) in the temperature from −70 to 80 °C under a nitrogen gas atmosphere. Thermogravimetric analysis (TGA) was carried out using a Simultaneous Thermal Analyzer (Mettler Toledo TGA/DSC 1). The samples were heated between 30 to 900 °C at a heating rate of 10 °C min^{-1} under a 40 mL min^{-1} nitrogen atmosphere. The mechanical properties of PU were evaluated by uniaxial tensile tests at 20 °C using an Instron 5566 universal tensile tester. The samples with a surface dimension of 40 × 6 mm^2 and a thickness of 2 mm were employed. The tension to break was applied with a rate of 10−100 mm min^{-1}. The self-healing properties of samples were also qualified by the tensile strength experiment. The dynamic mechanical analysis (DMA) was recorded using a PerkinElmer DMA 8000 by tension model from −80 to 50 °C (ramping rate = 5 °C min^{-1}). The specimens were cut into two pieces using histological blades and put in contact. Then the samples were left in air for a certain duration of experiment (from 5 to 1440 min).

3. RESULTS AND DISCUSSION

Commercial PEG-diol and PPG-triol, IPTG, and AHMP were selected as the key components to design the PU with tunable mechanical and self-healing properties. As shown in Scheme 1, an excess amount of IPDI was reacted with a dried mixture of PEG-diol and PPG-triol to form urethane *prepolymer 1*, which was capped with isocyanate (NCO) groups. Then a predetermined amount of AHMP was reacted with *prepolymer 1* to obtain the mixture of *prepolymer 2* containing partially UPy functional end-groups. Finally, stoichiometric BDO was added into *prepolymer 2* to react with the residual NCO groups to obtain PU-UPy.

3.1. Characterization. ATR-IR was used for monitoring the reaction process. As shown in Figure 1A, a broad shoulder

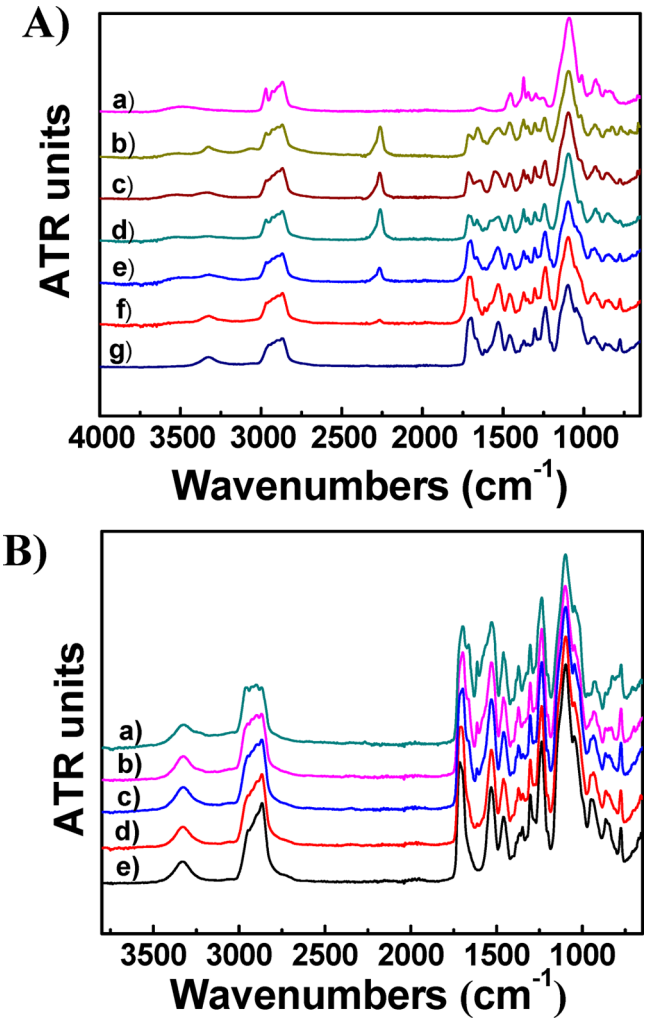


Figure 1. (A) FTIR spectra recorded at different time intervals for preparing PU1/5-AHMP-0.50: (a) mixture of PEG-diol and PPG-triol before adding IPDI; (b) 5 min and (c) 120 min after adding IPDI, respectively; (d) 30 min after mixing with AHMP; (e) 30 min, (f) 60 min, and (g) 120 min after adding BDO, respectively. (B) FTIR spectra of PU with various ratios of AHMP/PEG 1000: (a) PU1/5-AHMP-0; (b) PU1/5-AHMP-0.25; (c) PU1/5-AHMP-0.50; (d) PU1/5-AHMP-0.75; (e) PU1/5-AHMP-1.0. Nomenclature see the main text.

at 3327 cm^{-1} attributes to the stretching vibration of the −OH group of PEG-diol and PPG-triol, gradually shifts to the high field region due to the formation of urethane. This vibration can also be confirmed by the decrease of peak intensity at 2263 cm^{-1}, which belongs to the isocyanate stretching vibration after successively adding AHMP and BDO. This peak eventually disappears after incubating for 2 h in the oven at 100 °C. The appearance of a new peak at 1715 cm^{-1} is attributed to the C=O stretching vibration of urethane, which increases with the

DOI: 10.1021/acsapm.8b00153
ACS Appl. Polym. Mater. 2019, 1, 425−436

reaction time and also demonstrates the successful formation of the urethane bond. FTIR after addition of different ratios of AHMP was also investigated and as shown in Figure 1B, the peaks at 2957 and 1612 cm^{-1}, which correspond to the methyl and C=O stretching vibration of UPy group, respectively, increase with the feeding ratio of [AHMP]/[PEG 1000], confirming the incorporation of UPy group in the polymer matrix.

The thermal stabilities of as-prepared samples were evaluated using TGA and shown in Figure 2. Here, for

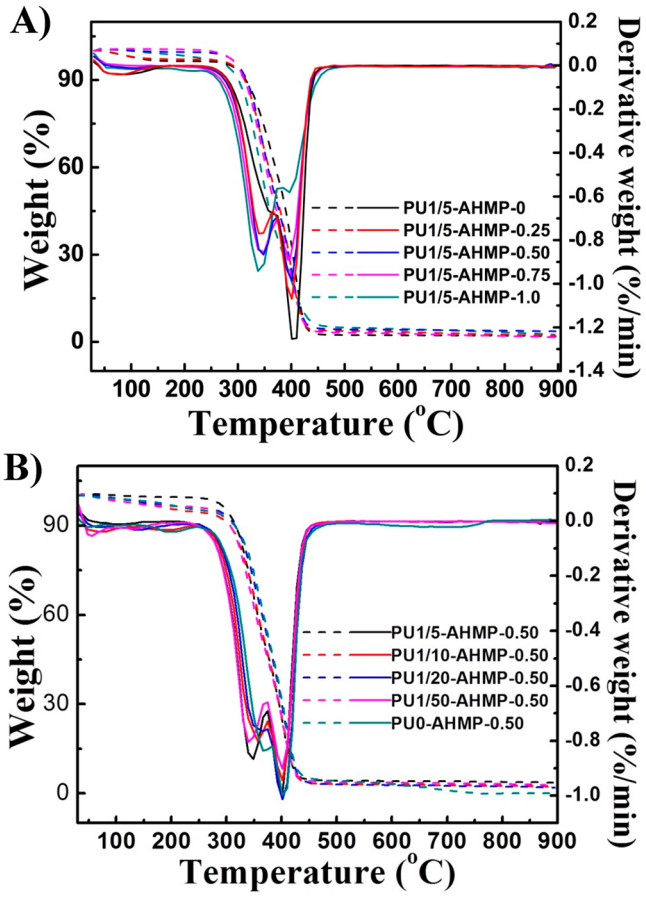


Figure 2. Thermogravimetric analysis (TGA) of PU (A) containing differenct feeding ratios of AHMP and (B) different feeding ratio of PPG-triol.

simplicity we name samples according to their PU and ANMP contents. For example, PU1/5-AHMP-0.25 means the molar ratio of −OH hydroxyl groups of PEG-diol to PPG-triol is 1:5, while 0.25 is the molar ratio of the total −OH and $-NH_2$ groups from AHMP to the total −OH groups from PEG-diol and PPG-triol. The PU1/5-AHMP-0 without any UPy motifs displays almost a unimodal TGA derivative profile with a single peak at 397.4 °C. We anticipate certain thermal stability changes upon modification with the Upy motifs, which was investigated with TGA experiments. As is evident in the data, the bimodal peaks obviously appeared in the range of 339.9−349.5 °C and at 397.4 °C corresponding to the elimination of UPy units and degradation of polyols. The degradation degree of the first degradation step increases with the feeding ratio of AHMP during the synthesis process. Specifically, the undecomposed weight ratio at 365 °C decrease from 63.1% for PU1/5-AHMP-0 to 40.9% for PU1/5-AHMP-1.0, respectively. These results demonstrate that the existence of UPys motifs can slightly decrease the thermostability of samples to some extent.[73] Further elevating temperature results the decomposition of the PU backbone.[57] Increasing the feeding ratios of PPG-triol/PEG-diol also exhibits similar degradation profiles (Figure 2B), wherein the first degradation of samples declines with the increase in PPG-triol. These features demonstrate the thermostability of as-prepared PU decreases with the introduction of UPy motifs and the PPG segment.

The glass transition temperatures (T_g) were investigated by DSC at a heating rate of 10 °C min^{-1} (Figure 3). Compared to

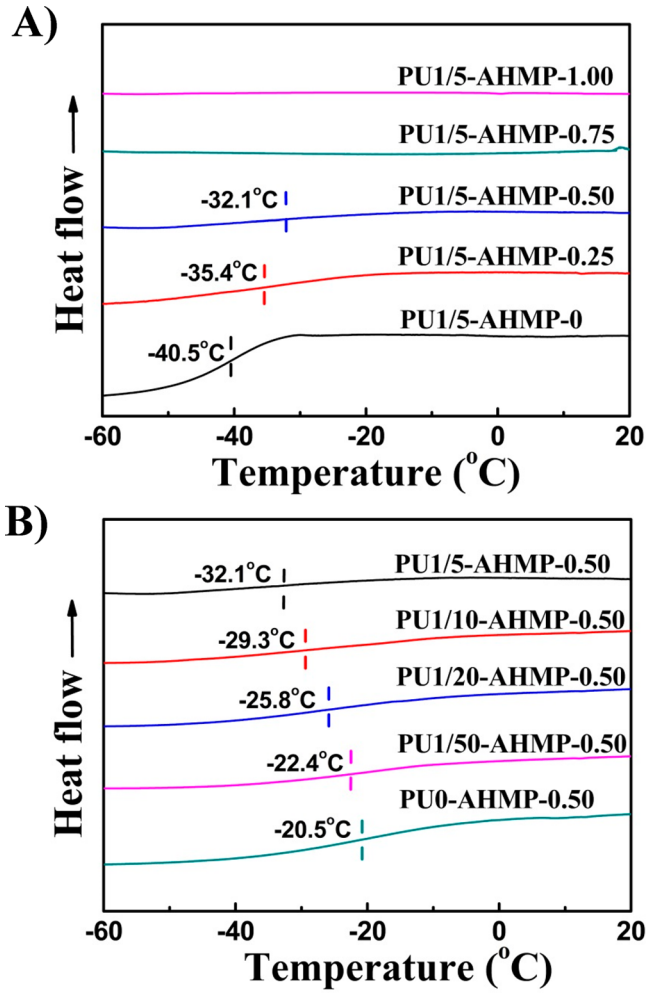


Figure 3. (A) DSC curves of PU with various ratios of AHMP/PEG 1000 and (B) DSC curves of PU with different feeding ratio of PPG.

the obvious crystallization behavior of pure PEG 1000 (Figure S1A), the as-prepared PU1/5-AHMP-0 has almost no crystallization peak but exhibits the obvious T_g at about −40.5 °C, indicating the structural regularity of pure PEG chain is disturbed by the hydrogen bonding between the −OH groups of PPG-triol and PEG-diol as well as the isocyanate group of IPDI.[74] However, the T_g of samples with increased AHMP contents (PU1/5-AHMP-0.25 VS PU1/5-AHMP-0.50) increases from −35.4 °C to −32.1 °C and eventually disappears at high AHMP contents such as PU1/5-AHMP-0.75 and PU1/5-AHMP-1.0. The subzero T_gs of those PUs can also be confirmed by DMA, as shown in Figure S3. For

DOI: 10.1021/acsapm.8b00153
ACS Appl. Polym. Mater. 2019, 1, 425−436

example, the T_g of PU1/5-AHMP-0.50, estimated from the maximum loss modulus of E'', is ~45.7 °C, which demonstrates the T_g obtained from DSC is reasonable. For the samples containing different amount of PPG, for example, the T_g of PU1/10-AHMP-0.50, PU1/20-AHMP-0.50, PU1/50-AHMP-0.50, and PU0-AHMP-0.50 is −29.3, −25.8, −22.4 °C, and −20.5 °C, respectively, implying that PPG in polymer matrix results in a decrease in T_g to a certain extent. This is reasonable because of the noncrystallization nature of PPG-3000 in the tested temperature range (−70 to 80 °C, Figure S1B). Notably, T_g of all samples are far below room temperature, indicating polymer chains at room temperature can move freely. This is a typical characteristic of most polymers or composites with room-temperature self-healing properties wherein nonequilibrium states of polymer chain can be reversed to the equilibrium states via chain movement.[1]

3.2. Mechanical Properties of PUs. In general, the mechanical property is one of key factors that determines the practical application of materials.[75,76] In here, tensile tests were performed at room temperature to investigate the basic mechanical properties of as the prepared PU. As shown in Figure 4A, the PU1/5-AHMP-0 without the UPy motifs exhibits a typical elastomer profile,[77] and the Young's modulus, maximum load, and elastic deformation are 1.86 ± 0.16 MPa, 5.12 ± 0.13 MPa, and 1147% ± 93%, respectively. Notably, after the sample underwent a large deformation, it could recover back to its original shape within a few seconds once removing the tensile stress.[11] Upon introduction of the UPy motifs, the mechanical property of samples is obviously influenced. For example, in comparison with the PU1/5-AHMP-0 without UPy motifs, the PU1/5-AHMP-0.25, containing a small amount of UPy motifs, possesses relative lower Young's modulus and maximum stress (1.58 ± 0.30 MPa and 1.24 ± 0.12 MPa, respectively), although the elongation at break is relatively high (1287% ± 42%). Further increase in the content of AHMP led to an increase in the mechanical property as well as the elongation at break. For example, the Young's modulus, elongation at break, and maximum stress of PU1/5-AHMP-0.50 are 3.02 ± 0.10 MPa, 1508% ± 85% and 1.93 ± 0.13 MPa, respectively. It is noted that an excess content of AHMP results in an improvement of mechanical properties, whereas a decrease of the elongation at break is seen. For example, the Young's modulus values of PU1/5-AHMP-0.75 and PU1/5-AHMP-1.0 are 5.51 ± 0.34 and 23.89 ± 1.32 MPa, respectively, the elongation at break of samples decreased to 873% ± 69% for PU1/5-AHMP-0.75 and 4% ± 0.1% for PU1/5-AHMP-1.0, respectively, and the maximum stress is 6.47 ± 0.27 and 2.88 ± 0.11 MPa, respectively. As is evident in Figure S5, the trend obtained from the true stress-true strain curve is similar to the static stress−strain profile shown in Figure 4A. These features demonstrate that UPy motifs are very efficient on tuning the mechanical properties of as-prepared PU and modest contents of UPy motifs endow the samples with good mechanical properties as well as excellent elongation at break, while higher contents of that significantly decrease the elongation at break of the sample, which yields fragile plastics.

The effect of macromolecular cross-linker PPG-triol on the mechanical properties of PU was also investigated. As shown in Figure 4B and Table 1, the Young's modulus of as-prepared samples decreases from 3.08 ± 0.28 MPa for PU1/5-AHMP-0.50 to 1.16 ± 0.05 MPa for PU0-AHMP-0.50, while the elongation at break changes from 1508 ± 85% for PU1/5-AHMP-0.50 to 3098 ± 158% for PU0-AHMP-0.50, respectively, demonstrating that the incorporation of PPG-triol slightly improves the mechanical properties of as-prepared PU while it decreases the elongation at break. Notably, the ultimate strength at break of samples decreases from 1.93 ± 0.13 MPa to 0.02 ± 0.01 MPa with a decrease in AHMP content. The influence of tensile rate on mechanical properties

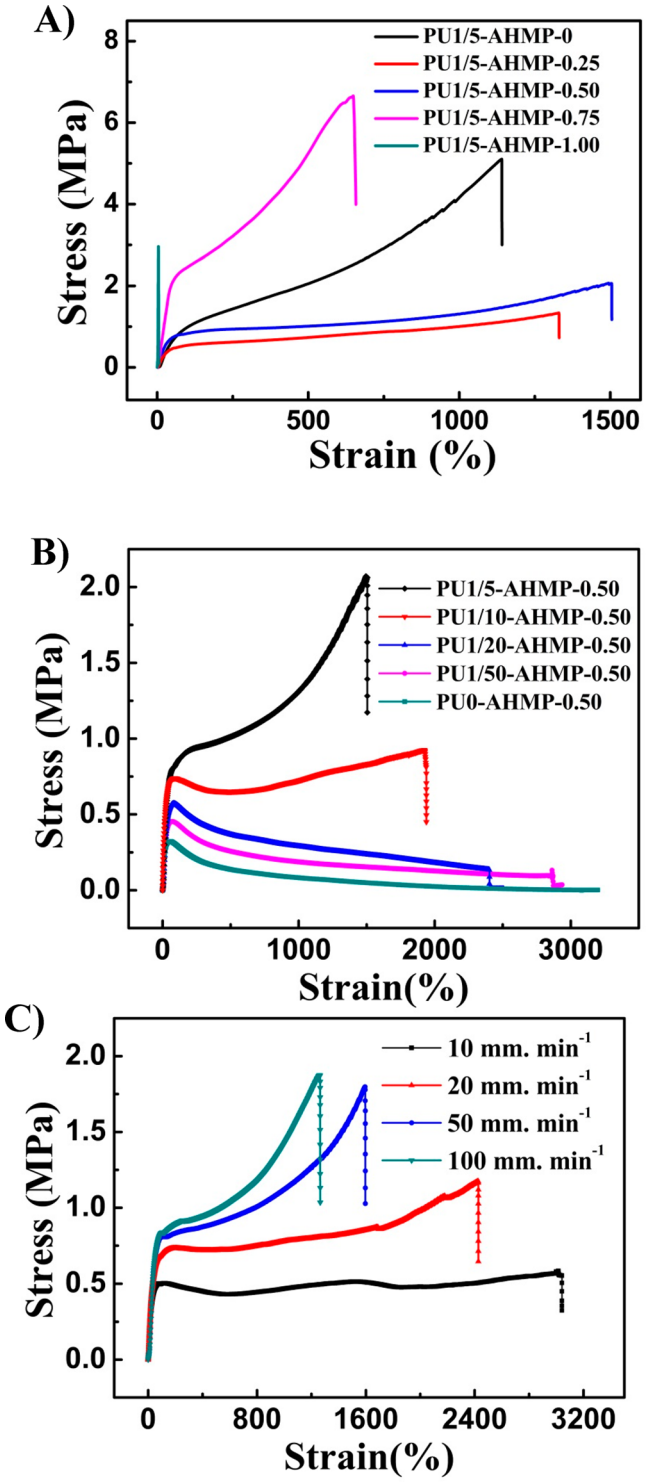


Figure 4. Static tensile tests of PU (A) with various feeding ratios of AHMP (strain rate = 100 mm min^{-1}), (B) various PPG triol contents (strain rate = 100 mm min^{-1}), and (C) PU1/5-AHMP-0.50 at the different tensile rates.

DOI: 10.1021/acsapm.8b00153
ACS Appl. Polym. Mater. 2019, 1, 425−436

Table 1. Mechanical Properties of Self-Healing PUs with Different Compositions

	original			after healing (1440 min)	
sample	E (Mpa)	ε_{break} (%)	δ_{break} (Mpa)	ε_{break} (%)	δ_{break} (Mpa)
PU1/5-AHMP-0	1.86 ± 0.16	1147 ± 93	5.12 ± 0.13		
PU1/5-AHMP-0.25	1.58 ± 0.30	1286 ± 42	1.24 ± 0.12	1132 ± 61	1.06 ± 0.15
PU1/5-AHMP-0.50	3.02 ± 0.10	1508 ± 85	1.93 ± 0.13	1460 ± 44	1.78 ± 0.11
PU1/5-AHMP-0.75	5.51 ± 0.34	873 ± 68	6.47 ± 0.27	640 ± 23	3.03 ± 0.24
PU1/5-AHMP-1.0	23.89 ± 1.32	4 ± 0.1	5.12 ± 0.13		
PU1/10-AHMP-0.50	2.73 ± 0.08	1969 ± 69	1.08 ± 0.17		
PU1/20-AHMP-0.50	1.89 ± 0.01	2353 ± 62	0.16 ± 0.04		
PU1/50-AHMP-0.50	1.58 ± 0.10	2901 ± 105	0.09 ± 0.01		
PU0-AHMP-0.50	1.16 ± 0.05	3098 ± 158	0.02 ± 0.01		

was investigated using PU1/5-AHMP-0.5, and the results demonstrate that the mechanical strength increases from 0.57 ± 0.17 MPa to 1.18 ± 0.10 MPa with the an increase in tensile speed from 10 mm min^{-1} to 100 mm min^{-1}, while the corresponding elongation at break decreases from 3019 ± 22% to 1252 ± 17%, indicating samples with appropriate contents of UPy in PU matrix can exhibit excellent tensile properties. Notably, postpeak strain softening behavior can be observed for samples with relatively lower feeding ratios of PPG-trio, which has a positive effect on increasing the samples' mechanical properties and enhancing the elastomer characteristics.

To further evaluate our samples' mechanical performance, we selected PU1/5-AHMP-0.50 as an example to demonstrate the cyclic tensile loading−unloading experiments. As shown in Figure S6, large hysteresis loops were observed during cyclic tensile loading−unloading experiments without any rest time between adjacent cycles. The tensional stress of the second cycle is apparently lower than that of the first one for the initial three cycles. The hysteresis ratio decreases from 65.5 for the first cycle to 57.1% for the fourth cycle. This feature indicates that the PU1/5-AHMP-0.50 can effectively dissipate energy[78] and exhibits excellent mechanical properties.

The tunable mechanical properties of samples are attributed to the existence of UPy motifs in the polymer matrix. Specifically, for samples with lower content of AHMP, the existence of small amount of UPy groups at the ends of polymer chains could effectively decrease the molecular weight as well as the cross-linking degree of samples. This reduction can be confirmed from the swelling behavior of samples in good solvents (such as dimethylacetamide (DMAc) and tetrahydrofuran (THF)). For example, in comparison with the visibly swollen of PU1/5-AHMP-0, PU1/5-AHMP-0.25 displays relatively higher swelling degree in those DMAc and THF. The leaching solution of PU1/5-AHMP-0.25 could form thin membrane after evaporation of solvents, indicating there is a certain degree of non-cross-linked network of PU1/5-AHMP-0.25. However, further increase the content of AHMP results in samples with excellent solubility in aforementioned solvents. For example, PU1/5-AHMP-0.50, PU1/5-AHMP-0.75, and PU1/5-AHMP-1.0 can be totally dissolved in those solvents. Furthermore, transparent solutions can be obtained after heating in those solvents, indicating that the UPy capping of polymer chains decreases the molecular weight because the terminate UPy groups can effectively block the formation of covalently cross-linked three-dimensional networks. On the other hand, the formation of quadruple hydrogen bonds aroused from the UPy groups could effectively enhance the interaction among polymer chains in the network and correspondingly the tensile strengths, although the decrease in molecular weight and cross-linking degree would compromise these values. The relative lower modulus and tensile strength of PU1/5-AHMP-0.25 as compared to the PU1/5-AHMP-0 is probably due to the decrease in molecular weight and degree of cross-linking due to the capping effects of a small amount of Upy groups, which form a low degree of quadruple hydrogen bonding interactions. In comparison to samples with higher UPy contents, PU1/5-AHMP-0.25 has lower mechanical properties because of the formation of less quadruple hydrogen bonds. This is essentially why PU1/5-AHMP-0 displays typical elastomer properties, while the samples with the highest content of AHMP exhibit brittle plastic properties. This result also demonstrates that as-prepared samples with higher contents of AHMP, such as PU1/5-AHMP-0.50, could be molded into a variety of shapes and sizes for various applications. It should be noted that the mechanical properties of the obtained samples increase with the feeding ratio of PPG. This is likely due to the formation of more entangle structures via macromolecular PPG as well as the UPy capped PPG. Taken together, based on the above results we suggest that the PU with desired mechanical properties, such as a higher modulus and a higher elongation at break could be designed by further tuning of the feeding ratio of AHMP and PPG.

The viscoelastic properties of the samples were investigated via frequency-sweep rheological measurements from low to high frequencies (0−100 rad s^{-1}) with the strain fixed at 1%, as shown in Figure 5A. However, for samples with relatively high content of AHMP, such as PU1/5-AHMP-0.50, the values of G' of the sample will gradually approach to the G'' with an increase in frequency; a cross at ω = 0.115 is observed, indicating a transition to a liquid regime. The G' of PU1/5-AHMP-0.50 rapidly increases and is eventually higher than that of PU1/5-AHMP-0.25 after ω > 6.234. This is reasonable because PU1/5-AHMP-0.50 is in solid state at high frequencies. This result can also be verified by the tensile tests wherein the Young's modulus as well as other rate-dependent mechanical properties of PU1/5-AHMP-0.50 are slightly higher than that of PU1/5-AHMP-0.25. The enhancement in mechanical properties of UPy motifs can also be confirmed by PU1/5-AHMP-0.75 with a relative higher content of AHMP, wherein the solid−liquid transition point shifts to a lower frequency at ω = 0.103. This is likely due to the existence of numerous UPy motifs in the polymer matrix, which facilitate the formation of the reversible cross-links. Therefore, the PU1/5-AHMP-0.75 possesses relative higher G' and G'' as well as obviously frequency dependence.

The effect of macromolecular cross-linking agent PPG-triol on the rheology properties was also investigated, as shown in

DOI: 10.1021/acsapm.8b00153
ACS Appl. Polym. Mater. 2019, 1, 425−436

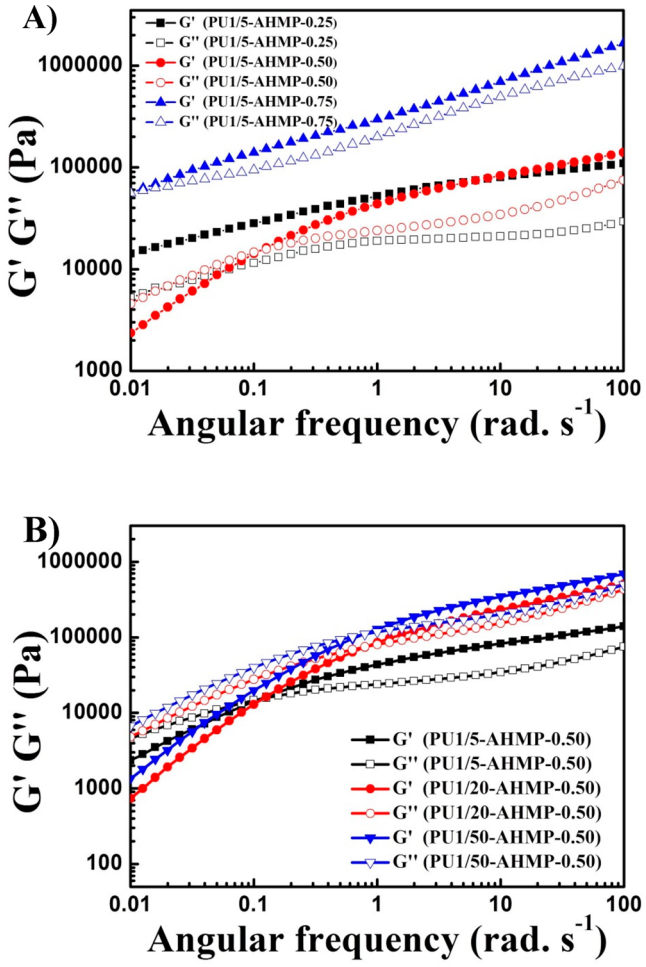


Figure 5. Storage modulus G' (solid) and loss modulus G'' (open) of with different feeding ratios of AHMP (a) and PPG (b).

Figure 5B. It is noted that all samples exhibit frequency dependency. Similar to the case of PU1/5-AHMP-0.50, the G' of samples gradually get close to the G'' with an increase in frequency, indicating the appearance of solid-like to liquid-like transition. Notably, the intersections of the G' and G'' frequency dependency of PU1/5-AHMP-0.50, PU1/20-AHMP-0.50, and PU1/50-AHMP-0.50 are at ω = 0.115, 0.787, and 0.836, respectively, indicating solid-like properties of samples upon decreasing in the feed ratio of PPG-triol.

3.3. Self-Healing Performances of PUs. In general, the relative low T_g is one of key factors for the amorphous polymers that could display self-healing properties at the room temperature.[12,79] The aforementioned results show that the crystallization peak of PEG 1000 disappears and all polyurethane except PU-AHMP-1.00 and PU1/5-AHMP-0.75 display subzero T_gs. For self-healing tests, samples were cut into two pieces using a histological blade. The two pieces were brought into contact, as shown in Figure 6 (details see Movie I). Compared with PU1/5-AHMP-0, which has no self-healing property, PU1/5-AHMP-5.0 displays excellent elongation at break, while the healed samples with different contact time (from 0 to 30 min) display relatively good elongation at break. Notably, after the contact time was extended to 30 min or even longer, some of the fracture position would not be the cut point, demonstrating the sample possesses excellent self-healing properties and the healing performances increases with the duration of contact. Those results indicate the existence of urethane linkage, which bestows the PUs relative weak hydrogen bond as compared to the UPy can not endue the sample with room-temperature self-healing performance in our case.

The tensile tester was further applied to investigate the self-healing properties of PU1/5-AHMP-0.25, PU1/5-AHMP-0.50, and PU1/5-AHMP-0.75. As shown in Figure 7, the elongation at break of PU1/5-AHMP-0.25, PU1/5-AHMP-0.50, and PU1/5-AHMP-0.75 after healing of 5 min is ~39.2%, 162%, and 14%, respectively, and corresponding healing efficiency is ~3%, 11%, and 1%, respectively. When the healing is beyond

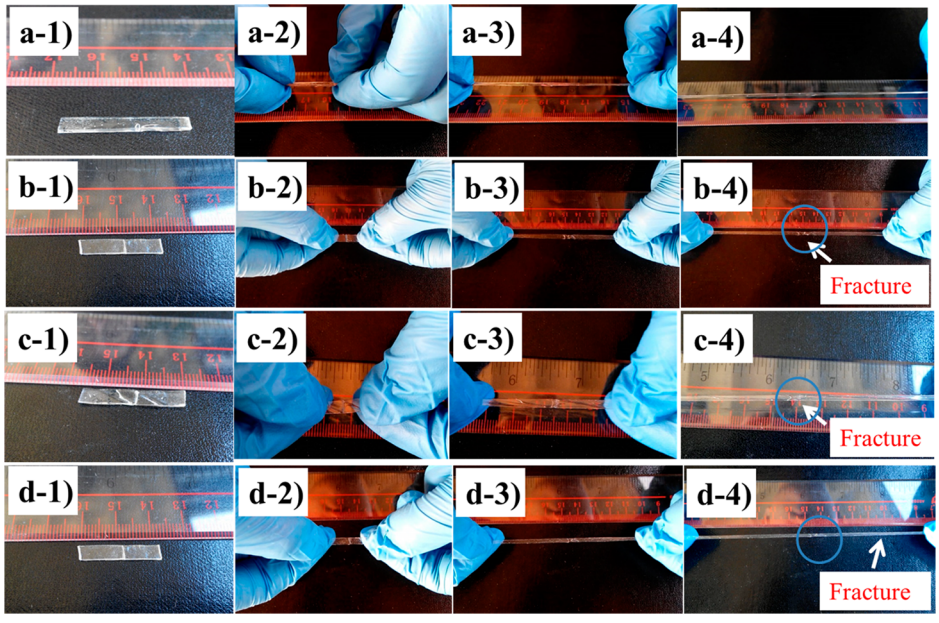


Figure 6. Snapshots showing the self-healing properties of PU1/5-AHMP-0.50 at room temperature: (a) original sample; (b) healing for 0 min; (c) healing for 5 min; and (d) healing for 30 min. 1−4 indicate different elongation.

DOI: 10.1021/acsapm.8b00153
ACS Appl. Polym. Mater. 2019, 1, 425−436

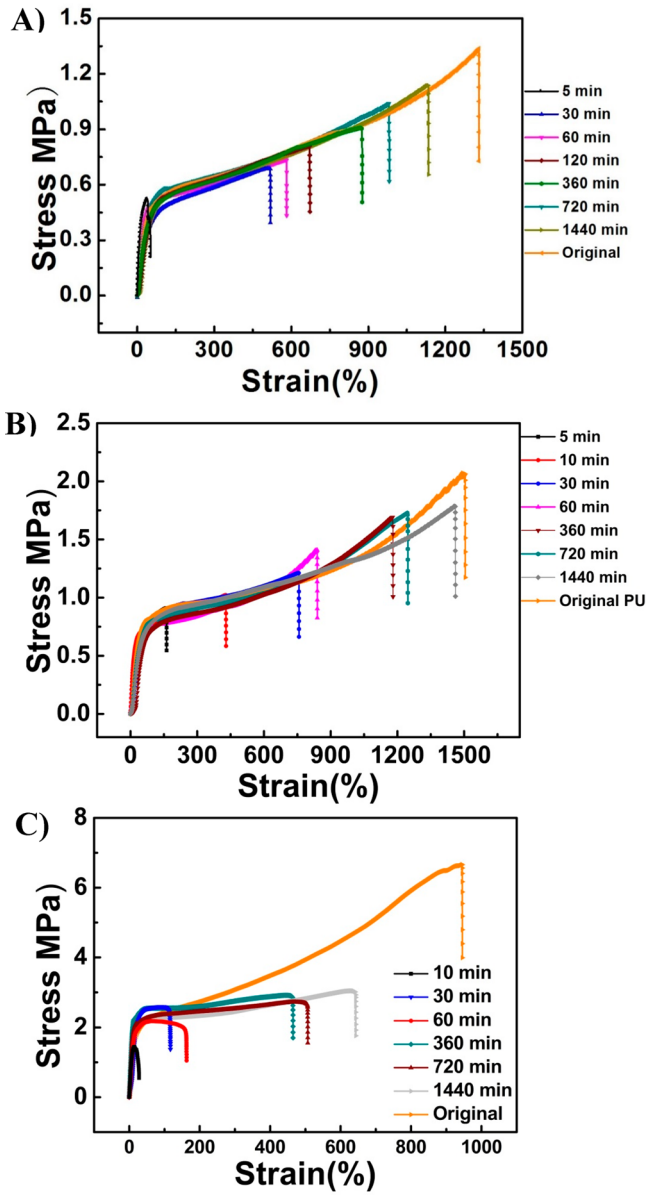


Figure 7. Typical strain−stress curves of as-prepared polyurethane (A) PU1/5-AHMP-0.25, (B) PU1/5-AHMP-0.50, and (C) PU1/5-AHMP-0.50 with different contact time ranging from 5 to 1440 min (12 h) at room temperature.

1440 min, the elongation at break is ∼1132%, 1460%, and 640%, and the corresponding healing efficiency is ∼88%, 97%, and 63%, respectively. This result indicates that PU1/5-AHMP-0.50 with a moderate content of AHMP possesses much better self-healing properties compared to PU1/5-AHMP-0.25 and PU1/5-AH MP-0.75. Notably, the broken pieces of samples could recover to the original structural integrity after contacting with each other for 12 h. These results also demonstrate that the self-healing properties of the samples initially increase with the content of AHMP. However, further increasing the content of AHMP results in an decrease in the healing efficiency. Eventually, a sample without self-healing properties was obtained, such as PU1/5-AHMP-1.0.

The effect of macromolecular PPG-triol on the self-healing properties of the PU samples was also evaluated via the uniaxial tensile tests. For samples with relative low feed ratios of PPG, the healing processes are much simpler. Samples, including PU1/10-AHMP-0.50, PU1/20-AHMP-0.50, and PU1/50-AHMP-0.50, reach almost total healing within 24 h. This result demonstrates that the self-healing properties of samples can be tuned by varying the contents of AHMP as well as PPG. Besides the elongation at break, the mechanical properties of healed samples are also key factors to evaluate the application of self-healing materials in the practical applications. As expected, the stain-stress curves of samples healed at different time are almost similar as the pristine sample. For example, the elongation at break of PU1/5-AHMP-0.50 at 5, 10, 30, 60, 120, 360, 720, and 1440 mm is ∼161%, 428%, 754%, 838%, 1178%, 1243%, and 1460%, respectively, and corresponding stress is ∼0.90, 1.02, 1.21,1.41,1.68,1.72, and 1.78 MPa, respectively. The stress of the original samples for the above strain is 0.90, 1.00, 1.14, 1.19, 1.52, 1.62, and 1.99 MPa, indicating the healed samples display excellent mechanical properties, which can also be observed from the samples with different contents of AHMP. Since the presence of UPy motifs in the polymer network could format reversible quadruple hydrogen bonds via donor−acceptor hydrogen interactions, a sample with a suitable AHMP content, such as PU1/5-AHMP-0.50, would display repeatable self-healing properties.

The self-healing process was also confirmed from optical microscope. As shown in Figure 8, the initial crack of PU1/50-AHMP-0.50 was gradually weakened and eventually disappeared after placing for 12 h at room temperature. However, this is not so obvious for PU1/5-AHMP-0.25 and PU1/5-AHMP-0.75, demonstrating the samples with moderated contents of AHMP possesses better self-healing property. However, the weakened scratches on the surface of PU1/5-AHMP-0.25 and PU1/5-AHMP-0.75 implied that these samples also possess certain self-healing characteristics at room temperature due to the slow chain motion.

In our work, the self-healing of our PUs does require manually contacting the two broken pieces, which makes it more scientifically a "self-healable" material. However, in the literature, almost all materials that are "self-healable" upon or without certain external stimuli are essentially called "self-healing" materials. We, therefore, follow such trends in this work.

3.4. Mechanism of Tunable Self-Healing. The tunable self-healing performances are likely attributed to the combined factors including the existence of UPy motifs in polymer matrix, the selection of PEG-diol and PPG-triol as polyethers, as well as IPDI as isocyanate. Specifically, the hydrogen interaction among urethane groups and the steric effect of the six-membered ring of IPDI could disturb the crystallization properties of pristine PEG segment;[80,81] the introduction of uncrystallized PPG-triol could decrease the T_g of as-obtained PU to some extent and the formed cross-linking networks could hinder chain movement at high PPG feeding ratios. These structural characteristics result in the polymer chain with sufficiently good movability at room temperature. Importantly, the capping effect of introduced UPy groups at the ends of polymer chains could effectively decrease the probability to form the intermolecular cross-linking structure as well as "freeze" further motion of polymer chains to some extent. Under very low Upy contents, the segment mobility is low due to a relatively high degree of cross-linking and H-bond density is low due to low Upy content. The self-healing capability is poor. That is why PU1/5-AHMP-0 exhibits typical elastomer characters without any self-healing ability, while PU1/5-AHMP-0.25 displays a slow self-healing property but

DOI: 10.1021/acsapm.8b00153
ACS Appl. Polym. Mater. 2019, 1, 425−436

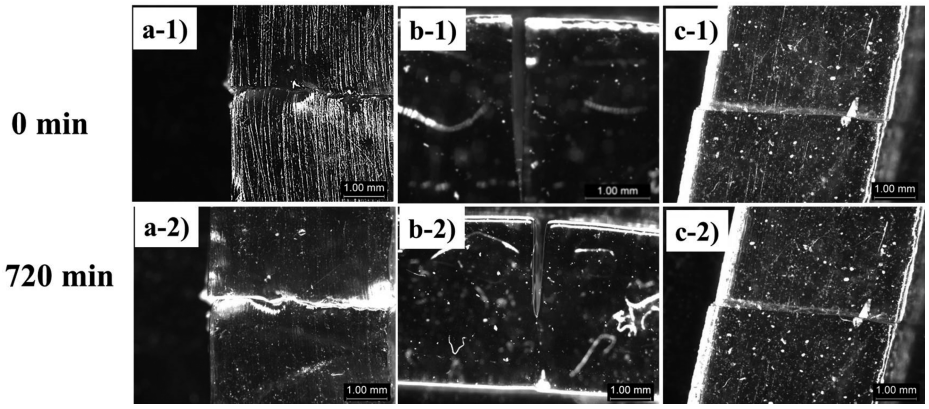


Figure 8. Optical microscope follow-ups of the self-healing of damaged samples (a) PU1/5-AHMP-0.25, (b) PU1/5-AHMP-0.50, and (c) PU1/5-AHMP-0.75 at room temperature for 0 (−1) and 720 (−2) min. Herein, "−1" and "−2" are used to distinguish the self-healing time of 0 and 720 min.

relatively low mechanical properties. A further increase in the content of the UPy motifs would yield a sample with a higher self-healing property because most end groups have been capped by UPys and there is almost no intermolecular cross-linking network. This fact facilitates the movement and rearrangement of polymer chains at ambient condition, while the strong quadruple hydrogen bonds aroused from relative higher UPy motif density bestow PU1/5-AHMP-0.50 excellent self-healing properties, as confirmed by the samples with low contents of PPG, such as PU1/10-AHMP-0.50 and PU0-AHMP-0.50. Indeed, too many UPy motifs in the polymer will restrict the movement of polymer chains as well as decrease the self-healing properties. Therefore, the samples containing moderated UPy contents could display the best self-healing properties. Under high Upy contents, the mobility is poor again due to the strong H-bonding interactions. The self-healing property is also poor. The performance of our PU1/5-AHMP-0.50 in comparison to pioneering self-healing works is summarized in Table 2. As is evident from the table, our materials show significantly increased breaking stress (and substantially decreased breaking strain) compared to other UPy based hydrogen bonding self-healing materials (row 1 of Table 2), which overall show enhanced performance. In comparison to regular hydrogen bonding self-healing materials (row 2 of Table 2), our materials show comparable breaking stress and breaking strain; however, our materials do not require external stimuli to induce self-healing. In comparison to other supplements needed self-healing materials (rows 3−5 of Table 2), our materials do not require chemical reagents feeding. Taken together, our work demonstrates the feasibility of preparing a material that can simultaneously satisfy the needs of self-healing and strong mechanical properties.

Table 2. Mechanical Property and Self-Healing Performance of Typical Room-Temperature Self-Healing Materials or Composites

mechanism	breaking stress	breaking strain (%)	time to reaches ~90% self-healing (h)	refs
hydrogen bond (UPy)	1.78	1460	12	this study
	0. 004	10 000	0.05	69
			0.08	70
			0.33	71
	0.27	~900	24	72
	0.38	2000	~0.16	62
hydrogen bond	~0.7	~270	12	48
	>2.5	>500	3	26
	~1.3	~1600	48	46
	~1.7	~700	24	47
metal−ligand interaction	~0.32	~1500	12	32
	~0.25	~1750	48	82
	~1.20	~780	3	31
disulfide bond	~0.4	~175	24	35
	~0.8	~2900	24	37
boronic esters	4.5	60	72	41
charge−charge interaction	~2.2	~630	12	40
host−guest interactions	0.5	~45	12	39
acylhydrazone	~0.25	~10 700	24	37
van der Waals	~4	~570	120	27
ion−dipole interactions	~ 0.2	~1500	24	38

4. CONCLUSIONS

To conclude, a series of PUs with tunable mechanical properties and room-temperature self-healing character was prepared via simply coupling of PEG-diol and PPG-triol and further incorporation of UPy motifs at the ends of polymer chains. Compared to samples without UPy motifs, which display typically elastomer characters with the Young's modulus of 1.86 ± 0.16 MPa and the elongation at break of 1147 ± 93%, the introduction of UPy motifs in the polymer matrix could effectively change their mechanical properties. For example, the Young's modulus increased from 1.58 ± 0.30 MPa for PU1/5-AHMP-0.25 to 23.89 ± 1.32 MPa for PU1/5-AHMP-1.0, and the elongation at break decreased from 1286 ± 42 to 4% ± 0.1%, respectively. It is noted that the samples with moderated contents of UPy motifs such as PU1/5-AHMP-0.75 display overall excellent mechanical properties such as relatively good Young's modulus (3.02 ± 0.10 MPa) and relatively good elongation at break at 1508 ± 85%. Results also demonstrate that the existence of appropriate PPG-triol contents could slightly increase the Young's modulus and decrease the elongation at break. Notably, the samples containing suitable UPy motifs such as PU1/5-AHMP-0.50 possess excellent room-temperature self-healing properties, wherein the cut samples could recover 11% only after a 5 min

DOI: 10.1021/acsapm.8b00153
ACS Appl. Polym. Mater. 2019, 1, 425−436

contact and 97% after a 1440 min contact, while samples with lower or higher UPy motifs only reaches 88% and 63% even after 1440 min. These results demonstrate the key role of thr UPy group in tuning the properties of as-prepared PU.

■ ASSOCIATED CONTENT

Supporting Information

The Supporting Information is available free of charge on the ACS Publications website at DOI: 10.1021/acsapm.8b00153.

Feed amount of reactant to prepare PU, DSC curves of PEG 1000 and PPG 3000 at rate, DSC profile of samples with wide temperature range, DMA results, true stress−strain curve, consecutive cyclic tensile loading−unloading curves, time-resolved FTIR spectra of PU1/5-AHMP-0.50 (PDF)

Self-healing performance video of PU1/5-AHMP-0.50 upon various contacting interval (AVI)

■ AUTHOR INFORMATION

Corresponding Author

*E-mail: tchujl@polyu.edu.hk.

ORCID

Jinlian Hu: 0000-0001-7084-8048

Zhongyu Yang: 0000-0002-3018-3608

Present Address

‡Institute of Textiles and Clothing, the Hong Kong Polytechnic University, Hong Kong 999077, China.

Notes

The authors declare no competing financial interest.

■ ACKNOWLEDGMENTS

The authors gratefully acknowledge the financial support from the National Natural Science Foundation of China (Grant No. 51673162) and the Hong Kong General Research Fund (RGC No. 15209815).

■ REFERENCES

(1) Yang, Y.; Urban, M. W. Self-Healing Polymeric Materials. *Chem. Soc. Rev.* **2013**, *42*, 7446−7467.

(2) Lutz, J.-F.; Lehn, J.-M.; Meijer, E. W.; Matyjaszewski, K. From Precision Polymers to Complex Materials and Systems. *Nat. Rev. Mater.* **2016**, *1*, 16024.

(3) Ghosh, B.; Urban, M. W. Self-Repairing Oxetane-Substituted Chitosan Polyurethane Networks. *Science* **2009**, *323*, 1458−1460.

(4) Wei, Z.; Yang, J. H.; Zhou, J.; Xu, F.; Zrínyi, M.; Dussault, P. H.; Osada, Y.; Chen, Y. M. Self-Healing Gels Based On Constitutional Dynamic Chemistry And Their Potential Applications. *Chem. Soc. Rev.* **2014**, *43*, 8114−8131.

(5) Lei, Z. Q.; Xiang, H. P.; Yuan, Y. J.; Rong, M. Z.; Zhang, M. Q. Room-Temperature Self-Healable and Remoldable Cross-linked Polymer Based on the Dynamic Exchange of Disulfide Bonds. *Chem. Mater.* **2014**, *26*, 2038−2046.

(6) Roy, N.; Bruchmann, B.; Lehn, J.-M. DYNAMERS: Dynamic Polymers as Self-Healing Materials. *Chem. Soc. Rev.* **2015**, *44*, 3786−3807.

(7) Taylor, D. L.; in het Panhuis, M. Self healing Hydrogels. *Adv. Mater.* **2016**, *28*, 9060−9093.

(8) Bai, Y.; Chen, Y.; Wang, Q.; Wang, T. Poly (Vinyl Butyral) Based Polymer Networks with Dual-Responsive Shape Memory and Self-Healing Properties. *J. Mater. Chem. A* **2014**, *2*, 9169−9177.

(9) Wang, D.; Guo, J.; Zhang, H.; Cheng, B.; Shen, H.; Zhao, N.; Xu, J. Intelligent Rubber with Tailored Properties for Self-Healing and Shape Memory. *J. Mater. Chem. A* **2015**, *3*, 12864−12872.

(10) Chen, S.; Mo, F.; Yang, Y.; Stadler, F. J.; Chen, S.; Yang, H.; Ge, Z. Development of Zwitterionic Polyurethanes with Multi-Shape Memory Effects and Self-Healing Properties. *J. Mater. Chem. A* **2015**, *3*, 2924−2933.

(11) Wang, C.; Liu, N.; Allen, R.; Tok, J. B. H.; Wu, Y.; Zhang, F.; Chen, Y.; Bao, Z. A Rapid and Efficient Self-Healing Thermo-Reversible Elastomer Crosslinked with Graphene Oxide. *Adv. Mater.* **2013**, *25*, 5785−5790.

(12) Tee, B. C. K.; Wang, C.; Allen, R.; Bao, Z. An Electrically and Mechanically Self-Healing Composite with Pressure- and Flexion-Sensitive Properties for Electronic Skin Applications. *Nat. Nanotechnol.* **2012**, *7*, 825−832.

(13) Chen, J.-Y.; Chen, X.-B.; Li, J.-L.; Tang, B.; Birbilis, N.; Wang, X. Electrosprayed PLGA Smart Containers for Active Anti-Corrosion Coating on Magnesium Alloy Amlite. *J. Mater. Chem. A* **2014**, *2*, 5738−5743.

(14) Fleet, E. J.; Zhang, Y.; Hayes, S. A.; Smith, P. J. Inkjet Printing of Self-Healing Polymers For Enhanced Composite Interlaminar Properties. *J. Mater. Chem. A* **2015**, *3*, 2283−2293.

(15) De Espinosa, L. M.; Fiore, G. L.; Weder, C.; Johan Foster, E.; Simon, Y. C. Healable Supramolecular Polymer Solids. *Prog. Polym. Sci.* **2015**, *49−50*, 60−78.

(16) Zhu, D. Y.; Rong, M. Z.; Zhang, M. Q. Self-Healing Polymeric Materials Based on Microencapsulated Healing Agents: from Design to Preparation. *Prog. Polym. Sci.* **2015**, *49−50*, 175−220.

(17) White, S. R.; Moore, J. S.; Sottos, N. R.; Krull, B. P.; Cruz, W. A. S.; Gergely, R. C. R. Restoration of Large Damage Volumes in Polymers. *Science* **2014**, *344*, 620−623.

(18) Sottos, N. R.; Moore, J. S. Materials Chemistry: Spot-on Healing. *Nature* **2011**, *472*, 299−300.

(19) Yin, T.; Zhou, L.; Rong, M. Z.; Zhang, M. Q. Self-Healing Woven Glass Fabric/Epoxy Composites with The Healant Consisting of Micro-Encapsulated Epoxy and Latent Curing Agent. *Smart Mater. Struct.* **2008**, *17*, 015019.

(20) Toohey, K. S.; Sottos, N. R.; Lewis, J. A.; Moore, J. S.; White, S. R. Self-Healing Materials with Microvascular Networks. *Nat. Mater.* **2007**, *6*, 581.

(21) Imato, K.; Nishihara, M.; Kanehara, T.; Amamoto, Y.; Takahara, A.; Otsuka, H. Self-Healing of Chemical Gels Cross-Linked by Diarylbibenzofuranone-Based Trigger-Free Dynamic Covalent Bonds at Room Temperature. *Angew. Chem., Int. Ed.* **2012**, *51*, 1138−1142.

(22) Deng, G.; Tang, C.; Li, F.; Jiang, H.; Chen, Y. Covalent Cross-Linked Polymer Gels with Reversible Sol− Gel Transition and Self-Healing Properties. *Macromolecules* **2010**, *43*, 1191−1194.

(23) Guo, M. Y.; Pitet, L. M.; Wyss, H. M.; Vos, M.; Dankers, P. Y. W.; Meijer, E. W. Tough Stimuli-Responsive Supramolecular Hydrogels with Hydrogen-Bonding Network Junctions. *J. Am. Chem. Soc.* **2014**, *136*, 6969−6977.

(24) Cordier, P.; Tournilhac, F.; Soulie-Ziakovic, C.; Leibler, L. Self-Healing and Thermoreversible Rubber from Supramolecular Assembly. *Nature* **2008**, *451*, 977−980.

(25) Phadke, A.; Zhang, C.; Arman, B.; Hsu, C.-C.; Mashelkar, R. A.; Lele, A. K.; Tauber, M. J.; Arya, G.; Varghese, S. Rapid Self-healing Hydrogels. *Proc. Natl. Acad. Sci. U. S. A.* **2012**, *109*, 4383−4388.

(26) Cordier, P.; Tournilhac, F.; Soulié-Ziakovic, C.; Leibler, L. Self-Healing and Thermoreversible Rubber from Supramolecular Assembly. *Nature* **2008**, *451*, 977−980.

(27) Bastings, M. M. C.; Koudstaal, S.; Kieltyka, R. E.; Nakano, Y.; Pape, A. C. H.; Feyen, D. A. M.; van Slochteren, F. J.; Doevendans, P. A.; Sluijter, J. P. G.; Meijer, E. W.; Chamuleau, S. A. J.; Dankers, P. Y. W. A Fast Ph-Switchable and Self-Healing Supramolecular Hydrogel Carrier for Guided, Local Catheter Injection in the Infarcted Myocardium. *Adv. Healthcare Mater.* **2014**, *3*, 70−78.

(28) Holten-Andersen, N.; Harrington, M. J.; Birkedal, H.; Lee, B. P.; Messersmith, P. B.; Lee, K. Y. C.; Waite, J. H. pH-Induced Metal-Ligand Cross-Links Inspired by Mussel Yield Self-Healing Polymer Networks with Near-Covalent Elastic Moduli. *Proc. Natl. Acad. Sci. U. S. A.* **2011**, *108*, 2651−2655.

(29) Mozhdehi, D.; Ayala, S.; Cromwell, O. R.; Guan, Z. Self-Healing Multiphase Polymers via Dynamic Metal−Ligand Interactions. *J. Am. Chem. Soc.* **2014**, *136*, 16128−16131.
(30) Faul, C. F. J.; Antonietti, M. Ionic Self-Assembly: Facile Synthesis of Supramolecular Materials. *Adv. Mater.* **2003**, *15*, 673−683.
(31) Mozhdehi, D.; Ayala, S.; Cromwell, O. R.; Guan, Z. Self-healing Multiphase Polymers via Dynamic Metal-Ligand Interactions. *J. Am. Chem. Soc.* **2014**, *136*, 16128−16131.
(32) Mei, J. F.; Jia, X. Y.; Lai, J. C.; Sun, Y.; Li, C. H.; Wu, J. H.; Cao, Y.; You, X. Z.; Bao, Z. A Highly Stretchable and Autonomous Self-Healing Polymer Based on Combination of Pt···Pt and $\pi-\pi$ Interactions. *Macromol. Rapid Commun.* **2016**, *37*, 1667−1675.
(33) Caraballo, R.; Rahm, M.; Vongvilai, P.; Brinck, T.; Ramstrom, O. Phosphine-catalyzed Disulfide Metathesis. *Chem. Commun.* **2008**, *48*, 6603−6605.
(34) Martin, R.; Rekondo, A.; Ruiz de Luzuriaga, A.; Cabanero, G.; Grande, H. J.; Odriozola, I. The Processability of A Poly(Urea-Urethane) Elastomer Reversibly Crosslinked With Aromatic Disulfide Bridges. *J. Mater. Chem. A* **2014**, *2*, 5710−5715.
(35) Amamoto, Y.; Otsuka, H.; Takahara, A.; Matyjaszewski, K. Self-Healing of Covalently Cross-Linked Polymers by Reshuffling Thiuram Disulfide Moieties in Air under Visible Light. *Adv. Mater.* **2012**, *24*, 3975−3980.
(36) Rekondo, A.; Martin, R.; Ruiz De Luzuriaga, A.; Cabañero, G.; Grande, H. J.; Odriozola, I. Catalyst-Free Room-Temperature Self-Healing Elastomers Based on Aromatic Disulfide Metathesis. *Mater. Horiz.* **2014**, *1*, 237−240.
(37) Wang, P.; Deng, G.; Zhou, L.; Li, Z.; Chen, Y. Ultrastretchable, Self-Healable Hydrogels Based on Dynamic Covalent Bonding and Triblock Copolymer Micellization. *ACS Macro Lett.* **2017**, *6*, 881−886.
(38) Cao, Y.; Morrissey, T. G.; Acome, E.; Allec, S. I.; Wong, B. M.; Keplinger, C.; Wang, C. A Transparent, Self-Healing, Highly Stretchable Ionic Conductor. *Adv. Mater.* **2017**, *29*, 1−9.
(39) Liu, J.; Tan, C. S. Y.; Yu, Z.; Li, N.; Abell, C.; Scherman, O. A. Tough Supramolecular Polymer Networks with Extreme Stretchability and Fast Room-Temperature Self-Healing. *Adv. Mater.* **2017**, *29*, 1−7.
(40) Luo, F.; Sun, T. L.; Nakajima, T.; Kurokawa, T.; Zhao, Y.; Sato, K.; Ihsan, A. B.; Li, X.; Guo, H.; Gong, J. P. Oppositely Charged Polyelectrolytes form Tough, Self-Healing, and Rebuildable Hydrogels. *Adv. Mater.* **2015**, *27*, 2722−2727.
(41) Cash, J. J.; Kubo, T.; Bapat, A. P.; Sumerlin, B. S. Room-Temperature Self-Healing Polymers Based on Dynamic-Covalent Boronic Esters. *Macromolecules* **2015**, *48*, 2098−2106.
(42) Burnworth, M.; Tang, L.; Kumpfer, J. R.; Duncan, A. J.; Beyer, F. L.; Fiore, G. L.; Rowan, S. J.; Weder, C. Optically Healable Supramolecular Polymers. *Nature* **2011**, *472*, 334−337.
(43) Wei, M.; Zhan, M.; Yu, D.; Xie, H.; He, M.; Yang, K.; Wang, Y. Novel Poly (Tetramethylene Ether) Glycol and Poly (E-Caprolactone) Based Dynamic Network via Quadruple Hydrogen Bonding with Triple-Shape Effect and Self-Healing Capacity. *ACS Appl. Mater. Interfaces* **2015**, *7*, 2585−2596.
(44) Hentschel, J.; Kushner, A. M.; Ziller, J.; Guan, Z. Self healing supramolecular block copolymers. *Angew. Chem.* **2012**, *124*, 10713−10717.
(45) Yu, C.; Wang, C. F.; Chen, S. Robust Self Healing Host−Guest Gels from Magnetocaloric Radical Polymerization. *Adv. Funct. Mater.* **2014**, *24*, 1235−1242.
(46) Kang, J.; Son, D.; Wang, G. J. N.; Liu, Y.; Lopez, J.; Kim, Y.; Oh, J. Y.; Katsumata, T.; Mun, J.; Lee, Y.; Jin, L.; Tok, J. B. H.; Bao, Z. Tough and Water-Insensitive Self-Healing Elastomer for Robust Electronic Skin. *Adv. Mater.* **2018**, *30*, 1−8.
(47) Chen, Y.; Kushner, A. M.; Williams, G. A.; Guan, Z. Multiphase Design of Autonomic Self-Healing Thermoplastic Elastomers. *Nat. Chem.* **2012**, *4*, 467−472.
(48) Ying, H.; Zhang, Y.; Cheng, J. Dynamic Urea Bond for the Design of Reversible and Self-Healing Polymers. *Nat. Commun.* **2014**, *5*, 1−9.
(49) Bao, C.; Jiang, Y. J.; Zhang, H.; Lu, X.; Sun, J. Room-Temperature Self-Healing and Recyclable Tough Polymer Composites Using Nitrogen-Coordinated Boroxines. *Adv. Funct. Mater.* **2018**, *28*, 1−10.
(50) Chen, S.; Mahmood, N.; Beiner, M.; Binder, W. H. Self Healing Materials from V and H Shaped Supramolecular Architectures. *Angew. Chem.* **2015**, *127*, 10326−10330.
(51) Dauber, P.; Hagler, A. T. Crystal Packing, Hydrogen Bonding, and the Effect of Crystal Forces on Molecular Conformation. *Acc. Chem. Res.* **1980**, *13*, 105−112.
(52) Tien, Y. I.; Wei, K. H. Hydrogen Bonding and Mechanical Properties in Segmented Montmorillonite/Polyurethane Nanocomposites of Different Hard Segment Ratios. *Polymer* **2001**, *42*, 3213−3221.
(53) Sijbesma, R. P.; Beijer, F. H.; Brunsveld, L.; Folmer, B. J. B.; Hirschberg, J. H. K. K.; Lange, R. F. M.; Lowe, J. K. L.; Meijer, E. W. Reversible Polymers Formed from Self-Complementary Monomers Using Quadruple Hydrogen Bonding. *Science* **1997**, *278*, 1601−1604.
(54) MacGillivray, L. R.; Atwood, J. L. Rational Design of Multi component Calix [4] arenes and Control of Their Alignment in the Solid State. *J. Am. Chem. Soc.* **1997**, *119*, 6931−6932.
(55) MacGillivray, L. R.; Atwood, J. L. A Chiral Spherical Molecular Assembly Held Together by 60 Hydrogen Bonds. *Nature* **1997**, *389*, 469−472.
(56) Sijbesma, R. P.; Beijer, F. H.; Brunsveld, L.; Folmer, B. J.; Hirschberg, J. K.; Lange, R. F.; Lowe, J. K.; Meijer, E. Reversible Polymers Formed from Self-Complementary Monomers Using Quadruple Hydrogen Bonding. *Science* **1997**, *278*, 1601−1604.
(57) Yamauchi, K.; Lizotte, J. R.; Long, T. E. Thermoreversible Poly(alkyl acrylates) Consisting of Self-Complementary Multiple Hydrogen Bonding. *Macromolecules* **2003**, *36*, 1083−1088.
(58) Folmer, B. J. B.; Sijbesma, R. P.; Versteegen, R. M.; van der Rijt, J. A. J.; Meijer, E. W. Supramolecular Polymer Materials: Chain Extension of Telechelic Polymers Using a Reactive Hydrogen-Bonding Synthon. *Adv. Mater.* **2000**, *12*, 874−878.
(59) Mansfeld, U.; Hager, M. D.; Hoogenboom, R.; Ott, C.; Winter, A.; Schubert, U. S. Advanced Supramolecular Initiator for Nitroxide-Mediated Polymerizations Containing Both Metal-Ion Coordination and Hydrogen-Bonding Sites. *Chem. Commun.* **2009**, *23*, 3386−3388.
(60) Biyani, M. V.; Foster, E. J.; Weder, C. Light-Healable Supramolecular Nanocomposites Based on Modified Cellulose Nanocrystals. *ACS Macro Lett.* **2013**, *2*, 236−240.
(61) Oya, N.; Ikezaki, T.; Yoshie, N. A Crystalline Supramolecular Polymer with Self-Healing Capability at Room Temperature. *Polym. J.* **2013**, *45*, 955−961.
(62) Han, J. T.; Jeong, B. H.; Seo, S. H.; Roh, K. C.; Kim, S.; Choi, S.; Woo, J. S.; Kim, H. Y.; Jang, J. I.; Shin, D.-C.; Jeong, S.; Jeong, H. J.; Jeong, S. Y.; Lee, G.-W. Dispersant-Free Conducting Pastes for Flexible and Printed Nanocarbon Electrodes. *Nat. Commun.* **2013**, *4*, 2491.
(63) Lin, Y.; Li, G. An Intermolecular Quadruple Hydrogen-Bonding Strategy to Fabricate Self-Healing and Highly Deformable Polyurethane Hydrogels. *J. Mater. Chem. B* **2014**, *2*, 6878−6885.
(64) Teunissen, A. J. P.; Nieuwenhuizen, M. M. L.; Rodríguez-Llansola, F.; Palmans, A. R. A.; Meijer, E. W. Mechanically Induced Gelation of a Kinetically Trapped Supramolecular Polymer. *Macromolecules* **2014**, *47*, 8429−8436.
(65) Bobade, S. L.; Malmgren, T.; Baskaran, D. Micellar-Cluster Association OF Ureidopyrimidone Functionalized Monochelic Polybutadiene. *Polym. Chem.* **2014**, *5*, 910−920.
(66) Wei, M.; Zhan, M.; Yu, D.; Xie, H.; He, M.; Yang, K.; Wang, Y. Novel Poly(tetramethylene ether)glycol and Poly(ϵ-caprolactone) Based Dynamic Network via Quadruple Hydrogen Bonding with Triple-Shape Effect and Self-Healing Capacity. *ACS Appl. Mater. Interfaces* **2015**, *7*, 2585−2596.
(67) Song, Y.; Liu, Y.; Qi, T.; Li, G. L. Towards Dynamic but Supertough Healable Polymers through Biomimetic Hierarchical Hydrogen Bonding Interactions. *Angew. Chem., Int. Ed.* **2018**, *57*, 13838−13842.

DOI: 10.1021/acsapm.8b00153
ACS Appl. Polym. Mater. 2019, 1, 425−436

(68) Monemian, S.; Jang, K.-S.; Ghassemi, H.; Korley, L. T. J. Probing the Interplay of Ultraviolet Cross-Linking and Noncovalent Interactions in Supramolecular Elastomers. *Macromolecules* **2014**, *47*, 5633−5642.
(69) Jeon, I.; Cui, J.; Illeperuma, W. R. K.; Aizenberg, J.; Vlassak, J. J. Extremely Stretchable and Fast Self-Healing Hydrogels. *Adv. Mater.* **2016**, *28*, 4678−4683.
(70) Cui, J.; del Campo, A. Multivalent H-Bonds for Self-Healing Hydrogels. *Chem. Commun.* **2012**, *48*, 9302−9304.
(71) Zhu, D.; Ye, Q.; Lu, X.; Lu, Q. Self-Healing Polymers with PEG Oligomer Side Chains Based on Multiple H-Bonding and Adhesion Properties. *Polym. Chem.* **2015**, *6*, 5086−5092.
(72) Chen, S.; Mahmood, N.; Beiner, M.; Binder, W. H. Self-Healing Materials from V- and H-Shaped Supramolecular Architectures. *Angew. Chem.* **2015**, *127*, 10326−10330.
(73) Zhu, B.; Feng, Z.; Zheng, Z.; Wang, X. Thermoreversible Supramolecular Polyurethanes with Self-Complementary Quadruple Hydrogen-Bonded End Groups. *J. Appl. Polym. Sci.* **2012**, *123*, 1755−1763.
(74) Oprea, S. Effect of the Long Chain Extender on the Properties of Linear and Castor Oil Cross-Linked PEG-Based Polyurethane Elastomers. *J. Mater. Sci.* **2011**, *46*, 2251−2258.
(75) Williams, G. A.; Ishige, R.; Cromwell, O. R.; Chung, J.; Takahara, A.; Guan, Z. Mechanically Robust and Self-Healable Superlattice Nanocomposites by Self-Assembly of Single-Component "Sticky" Polymer-Grafted Nanoparticles. *Adv. Mater.* **2015**, *27*, 3934−3941.
(76) Xie, T. Tunable Polymer Multi-Shape Memory Effect. *Nature* **2010**, *464*, 267−270.
(77) Chen, Y.; Kushner, A. M.; Williams, G. A.; Guan, Z. Multiphase Design of Autonomic Self-Healing Thermoplastic Elastomers. *Nat. Chem.* **2012**, *4*, 467−472.
(78) Sun, J.-Y.; Zhao, X.; Illeperuma, W. R.; Chaudhuri, O.; Oh, K. H.; Mooney, D. J.; Vlassak, J. J.; Suo, Z. Highly Stretchable and Tough Hydrogels. *Nature* **2012**, *489*, 133.
(79) Wang, C.; Wu, H.; Chen, Z.; McDowell, M. T.; Cui, Y.; Bao, Z. Self-Healing Chemistry Enables the Stable Operation of Silicon Microparticle Anodes for High-Energy Lithium-Ion Batteries. *Nat. Chem.* **2013**, *5*, 1042−1048.
(80) Uemura, T.; Yanai, N.; Watanabe, S.; Tanaka, H.; Numaguchi, R.; Miyahara, M. T.; Ohta, Y.; Nagaoka, M.; Kitagawa, S. Unveiling Thermal Transitions of Polymers in Subnanometre Pores. *Nat. Commun.* **2010**, *1*, 83.
(81) Mo, F.; Zhou, F.; Chen, S.; Yang, H.; Ge, Z.; Chen, S. Development of Shape Memory Polyurethane Based on Polyethylene Glycol and Liquefied 4,4′-Diphenylmethane Diisocyanate Using a Bulk Method for Biomedical Applications. *Polym. Int.* **2015**, *64*, 477−485.
(82) Li, C.-H.; Wang, C.; Keplinger, C.; Zuo, J.-L.; Jin, L.; Sun, Y.; Zheng, P.; Cao, Y.; Lissel, F.; Linder, C.; et al. A Highly Stretchable Autonomous Self-Healing Elastomer. *Nat. Chem.* **2016**, *8*, 618.

DOI: 10.1021/acsapm.8b00153
ACS Appl. Polym. Mater. 2019, 1, 425−436